processes associated with charge transfer when the dominant mode of mass transport is diffusion. In addition, concentration profiles for electromigration or turbulent conditions could be obtained, elucidating a variety of mass transport processes. Different electrode shapes, including microelectrodes, which have quite different diffusion profiles, are amenable to the same approach. Finally, the results demonstrate that absorbance is proportional to path length, so an electrode with a longer dimension along the optical axis will have higher sensitivity to the presence of chromophores. Unlike most spectroelectrochemical measurements, where effective path length is dictated by the diffusion process, the diffractive approach allows sampling of distances close to the electrode so long paths can be employed.

Given the theoretical basis of diffractive spectroelectrochemistry, future efforts will be directed toward establishing the practical limits on electrode length, time resolution, and sensitivity. In addition, the inversion process producing a diffusion profile shape from a diffraction pattern will be examined. The improved speed, sensitivity, and information content of the diffractive approach should significantly increase the generality of spectroelectrochemical techniques.

Acknowledgment. This work was supported by grants from NSF (CHE-7828068) and NIMH (24812).

Two-Dimensional Rotational Spin–Echo Nuclear Magnetic Resonance in Solids: Correlation of Chemical Shift and Dipolar Interactions

M. G. Munowitz,[1a] R. G. Griffin,*[1b] G. Bodenhausen,[1b,c] and T. H. Huang[1b]

Contribution from the Francis Bitter National Magnet Laboratory, Massachusetts Institute of Technology, Cambridge, Massachusetts 02139, and Department of Chemistry, Harvard University, Cambridge, Massachusetts 02138. Received August 11, 1980

Abstract: Two-dimensional NMR techniques which separate the chemical shift and heteronuclear dipolar interactions are applied to samples spinning at the magic angle. Because of the inhomogeneous nature of the two interactions, rotational echoes are observed in the time domain of each dimension. The corresponding Fourier transforms yield rotational sideband spectra which provide information on the principal values and relative orientations of the shift and dipolar tensors, and, from the latter, internuclear distances may be calculated. The techniques therefore provide a means for obtaining structural data, for example, ^{13}C–^{1}H and ^{15}N–^{1}H distances, in powder samples.

I. Introduction

One of the principal aims of high-resolution, solid-state NMR techniques is the suppression of homo- and heteronuclear dipolar interactions and the recovery of underlying chemical shifts and scalar spin couplings. Nevertheless, the development of high-resolution methods has suggested ways whereby dipolar couplings may be retained, and since these interactions contain information on internuclear distances and directions, they are clearly of considerable chemical significance. A particularly simple example is the observation of dipolar splittings between magnetically dilute spin pairs such as ^{13}C–^{14}N or ^{13}C–^{13}C.[2-5] In these cases, the proton-decoupled ^{13}C spectra show dipolar splittings from adjacent ^{14}N or ^{13}C nuclei. In addition, it has been demonstrated that a number of other chemically interesting groups constitute magnetically dilute systems, two examples being ^{13}C–^{1}H and ^{14}N–^{1}H. In the case of ^{14}N, which possesses a quadrupole moment, the lines are dispersed over 10^5–10^6 Hz, and the ^{14}N–^{1}H couplings, which are of the order of 10–15 kHz, are easily seen in single crystal spectra as small splittings on well-separated resonances.[6] However, the situation where one interaction dominates the other is not commonly encountered. More often, for example, in ^{13}C–^{1}H spectra, the dispersion of shifts is approximately the same size as the heteronuclear dipolar interaction, and consequently there is considerable overlap in the spectra, particularly in polycrystalline samples.

The *separation* of chemical shift and heteronuclear dipolar interactions in the NMR spectra of single crystals has recently been the subject of a number of two-dimensional experiments.[7,8] These methods, which are applicable to other inhomogeneous interactions,[9] generally allow for the evolution of the dipolar Hamiltonian during an interval prior to a proton-decoupled sampling period. Chemical shift spectra obtained in this manner receive information from the dipolar Hamiltonian in the form of a modulation, and a second Fourier transformation[10] separates the two interactions. This experiment is also applicable to powder samples[11,12] but when overlap from magnetically inequivalent nuclei occurs, the spectra are difficult to interpret.

The separation of overlapping chemical shift powder spectra can be accomplished with magic angle sample spinning (MASS).[13,14] When the spinning speed greatly exceeds the

---

(1) (a) Harvard University; (b) Francis Bitter National Magnet Laboratory; (c) Laboratory for Physical Chemistry, ETH—Zentrum, CH-8092 Zurich, Switzerland.

(2) (a) R. G. Griffin, A. Pines, and J. S. Waugh, *J. Chem. Phys.*, **63**, 3676 (1975); (b) M. E. Stoll, R. W. Vaughan, R. B. Saillant, and T. Cole, *ibid.*, **61**, 2896 (1974).

(3) S. Kaplan, A. Pines, R. G. Griffin, and J. S. Waugh, *Chem. Phys. Lett.* **25**, 78 (1974).

(4) H. van Willigen, R. G. Griffin, and R. A. Haberkorn, *J. Chem. Phys.*, **67**, 5855 (1977).

(5) D. L. van der Hart, *J. Magn Reson.*, **24**, 467 (1976).

(6) R. E. Stark, R. A. Haberkorn, and R. G. Griffin, *J. Chem. Phys.*, **68**, 1996 (1978).

(7) R. K. Hester, J. L. Ackerman, B. L. Neff, and J. S. Waugh, *Phys. Rev. Lett.* **36**, 1081 (1976).

(8) E. F. Rybaczewski, B. L. Neff, J. S. Waugh, and J. S. Sherfinski, *J. Chem. Phys.*, **67**, 1231 (1977).

(9) G. Bodenhausen, R. E. Stark, D. J. Ruben, and R. G. Griffin, *Chem. Phys. Lett.* **67**, 424 (1979).

(10) W. P. Aue, E. Bartholdi, and R. R. Ernst, *J. Chem. Phys.*, **64**, 2229 (1976).

(11) M. E. Stoll, A. J. Vega, and R. W. Vaughan, *J. Chem. Phys.*, **65**, 4093 (1976).

(12) M. Linder, A. Hohener, and R. R. Ernst, *J. Chem. Phys.*, **73**, 4959 (1980).

0002-7863/81/1503-2529$01.25/0

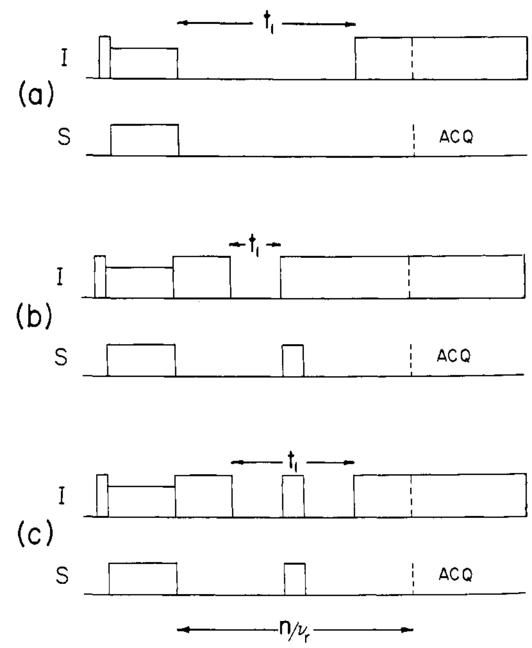

Figure 1. Pulse sequences which can be employed for two-dimensional rotational spin–echo spectroscopy. Common to all three sequences is the initiation of data acquisition at the peak of a rotational echo. Sequences b and c employ 180° refocusing pulses at the S and I frequencies, where $I = {}^1H$ and $S = {}^{13}C$ spins. The maximum evolution period in (b) is half that in (c). WAHUHA pulse trains during the t_1 period have been omitted for clarity. In (b) and (c) *n* must be even for refocusing to occur.

magnitude of the shift anisotropy, the spectrum consists of a single line at the isotropic resonance frequency of each magnetically inequivalent nucleus.[15] However, when the spinning speed is slow, the transient signal is composed of a train of rotational echoes spaced at multiples of the rotational period, and its Fourier transform yields a centerband flanked by sidebands spaced at the rotational frequency.[16-19] The success of the MASS experiment in this slow spinning regime is due to the fact that the chemical shift is an inhomogeneous interaction, and in fact MASS will suffice to narrow any interaction whose Hamiltonian satisfies this criterion.[17] For example, both first-order quadrupolar and heteronuclear dipolar interactions fall into this category. When two different inhomogeneous interactions are simultaneously present, they can be separated with a two-dimensional NMR experiment.[10] Thus, even in spinning powder samples it should be possible to extract and correlate high-resolution chemical shift and dipolar spectra. This paper describes three experiments which accomplish this separation. In particular, we outline methods which separate shift and heteronuclear dipolar powder spectra into two orthogonal frequency dimensions. In addition, we discuss in section IV a special case of these experiments, which is useful for differentiating between protonated and nonprotonated dilute spin resonances.

II. Rotationally Synchronized Pulse Sequences

Shown in Figure 1 are three pulse sequences which will separate the shift and dipolar interactions, where we denote by I and S the abundant (${}^1H$) and rare (${}^{13}C$) spins, respectively. Common to these sequences is the fact that the initiation of signal acquisition is always timed to coincide with the formation of a rotational spin–echo arising from the chemical shift. This is accomplished by restricting to a fixed integral number N of rotational periods the interval between preparation of the rare spins by cross polarization and the beginning of the acquisition. This feature is tantamount to refocusing the *anisotropic* part of the chemical shift, and ensures proper phase relationships among the rotational sidebands in both the chemical shift and dipolar domains. The evolution period, t_1, is simply defined as the time during which heteronuclear coupling is present. In pulse sequence 1a, the *isotropic* part of the S spin chemical shift is not refocused. For experiments which involve a single S spin resonance, such as are described below, this pulse sequence is perfectly adequate. However, for the common situation where more than a single line is present in the spectrum, use of sequence 1a will lead to substantial frequency-dependent phase shifts across the spectrum. These phase shifts arise because data acquisition commences an integral number of rotational periods after the cross polarization, a delay which is typically a few milliseconds. These frequency-dependent phase shifts can be circumvented by using either sequence 1b or 1c where 180° refocusing pulses are inserted into the experiment at the peak of the *n*th rotational echo, and data acquisition is commenced at the peak of the 2*n*th rotational echo. In 1b, the shift and dipolar Hamiltonians evolve together during t_1, but the dipolar part is decoupled after the refocusing pulse. The application of a 180° refocusing pulse to the S spins reverses the sign of S_z, and at the beginning of the signal acquisition there is no accumulated phase due to either the isotropic or anisotropic shift. Sequence 1c differs from 1b in that the heteronuclear dipolar coupling is allowed to act both before and after the refocusing pulse. Since the dipolar Hamiltonian is also linear in S_z it too would be refocused if a 180° pulse were applied to the S spins alone ($I_zS_z \rightarrow -I_zS_z$) and the dipolar evolution would not be transmitted to the second spectral dimension. This problem is easily avoided by the simultaneous application of 180° pulses to both species causing both terms in the Hamiltonian to reverse sign and the dipolar evolution to be preserved. Sequence 1c has the advantage that the maximum evolution period is twice that in 1b.

The line widths obtained in the dipolar or F_1 domain are largely determined by dipolar coupling among the protons. Hester et al.[7] and Stoll et al.[11] suggested the use of a multiple-pulse train to remove homonuclear interactions from the evolution period, and a simple WAHUHA sequence[20] serves dramatically to improve the resolution in this dimension. This is accomplished at the expense of a scaling of the heteronuclear dipolar interaction by a factor approximately equal to $3^{-1/2}$. The spectral width available in the dipolar dimension is intimately related to the WAHUHA cycle time. In practice we found it convenient to eliminate refocusing pulses (Figure 1a) in order to achieve a suitably dense sampling in t_1 while making most efficient use of the time available for evolution.

III. Chemical Shift - Dipolar Spectra

In the absence of sample rotation, the correlation between dipolar and chemical shift interactions is straightforward. For example, every point in an axially symmetric shift powder pattern corresponds to a known orientation of the unique axis ($\sigma_{\parallel}$) of the shift tensor relative to the magnetic field.[21,22] When a dipolar interaction is simultaneously present and the $\sigma_{\parallel}$ element of the shift tensor is along the internuclear vector, a two-dimensional experiment will produce a dipolar doublet for each value of the chemical shift. In particular, for $\sigma = \sigma_{\parallel}$, $D = D_{\parallel}$, for $\sigma = \sigma_{\perp}$, $D = -D_{\parallel}/2$, and for $\sigma = {}^1/_3\mathrm{Tr}(\tilde{\sigma})$, $D = 0$, where D refers to the dipolar splitting. The spectrum consists of two shift anisotropy powder patterns lying on the diagonals of the 2D plot. When viewed from the dipolar dimension, a Pake pattern is evident, while the projection onto the shift axis is the axially symmetric shift pattern.[12]

---

(13) E. R. Andrew, A. Bradbury, and R. G. Eades, *Nature (London)*, **182**, 1659 (1958).

(14) I. J. Lowe, *Phys. Rev. Lett.*, **2**, 285 (1959).

(15) J. Schaefer and E. O. Stejskal, *J. Am. Chem. Soc.*, **98**, 1031 (1976).

(16) E. Lippmaa, M. Alla, and T. Tuhem, Proceedings of The XIXth Ampere Congress, Heidelberg West Germany, 1976, p 113.

(17) M. Maricq and J. S. Waugh, *Chem. Phys. Lett.* **47**, 327 (1977); *J. Chem. Phys.*, **70**, 3300 (1979).

(18) J. Schaefer, E. O. Stejskal, and R. A. MacKay, *J. Magn. Reson.*, **25**, 569 (1977).

(19) R. A. Haberkorn, J. Herzfeld, and R. G. Griffin, *J. Am. Chem. Soc.*, **100**, 1296 (1978).

(20) J. S. Waugh, L. M. Huber, and U. Haeberlen, *Phys. Rev. Lett.* **20**, 180 (1968).

(21) U. Haeberlen, "High Resolution NMR in Solids", Academic Press, New York, 1976.

(22) M. Mehring, "NMR Basic Principles and Progress", Vol. II, Springer, New York, 1976.

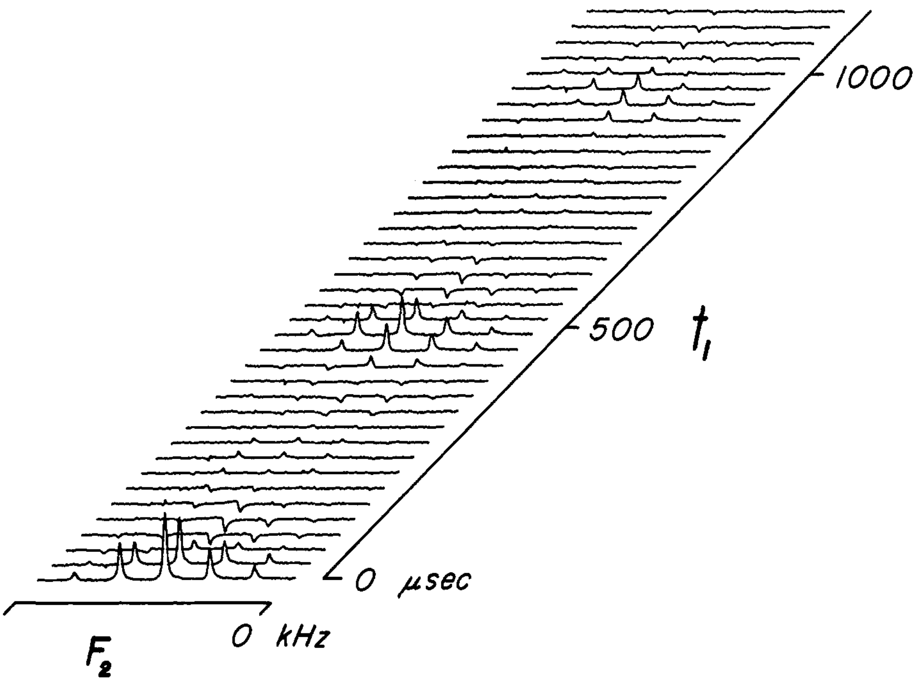

Figure 2. MASS spectra as a function of t_1 obtained from $Ca(CHO_2)_2$ using the pulse sequence in Figure 1a with WAHUHA in the evolution period. Modulation of the centerbands and sidebands in the chemical shift spectrum is due to the CH dipolar interaction.

In the case of a one-dimensional spinning experiment the clear association of resonant frequency with shift tensor orientation is lost when the spectrum is broken up into a collection of narrow sidebands. The sidebands are positioned at integer multiples of the rotation frequency as a consequence of the time dependence imparted to the Hamiltonian by the mechanical motion. The magnitude and phase of a sideband from a given crystallite are dependent on the orientation of the principal axis system in the reference frame of the rotor at the beginning of the pulse sequence. Different orientations contribute unequally to the various sidebands, and certain orientations may produce dispersive spectra. This has been observed for spinning single crystals.[17] When the $\sigma_{\parallel}$ element coincides with the rotor axis, the Hamiltonian remains time independent and the spectrum consists of a single line at the isotropic shift value, whereas when $\sigma_{\parallel}$ is perpendicular to the rotor axis all odd numbered sidebands are missing from the spectrum. For arbitrary orientations tilted with respect to the rotor axis, the rotation sweeps the spin packet through a range of resonant frequencies whose average always corresponds to the isotropic frequency. In a powder, a random set of orientations is present and the average over all positions leads to the familiar absorption-mode sideband spectrum.

In a two-dimensional spinning experiment involving two spin $^1/_2$ nuclei, the dipolar evolution introduces a modulation[23] of the chemical shift spectrum. Since the chemical shift and dipolar tensors are related by a molecule-fixed transformation, the magnitude of the peaks in the shift spectrum, corresponding to a given set of orientations, provides a measure of the contribution of an associated set of orientations to the dipolar spectrum. For example, when a sideband generated by a set of crystallites is purely dispersive or absent, there is nothing to modulate and no information is transmitted into the second spectral dimension. In the limit of vanishingly small shift anisotropy, each orientation contributes equally and suffers no phase shifts. Fourier transformation with respect to t_1 of the dipolar modulated centerband yields a Pake pattern split into sidebands. Such effects also occur when the spinning rates greatly exceed the shift anisotropy but remain comparable to the dipolar coupling. In this limit, the two-dimensional signals contain information about the magnitude of the dipolar couplings alone. When the spinner frequency is of the order of the shift anisotropy, the two-dimensional spectrum contains information about the relative orientation of the dipolar and shift principal axis system as well as the magnitude of the dipolar coupling as will be shown in a more detailed study. Since the dipolar tensor is traceless, symmetric, and aligned along an internuclear vector, information about relative orientations allows us to relate the chemical shift tensor to the molecular frame without the need for single-crystal studies.

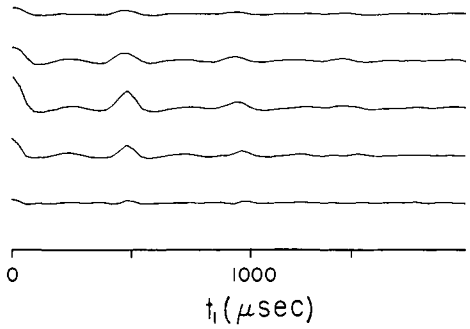

Figure 3. Plots of the centerband and sideband maxima of Figure 2 as a function of t_1 which show the occurrence of dipolar rotational echoes every spinner period (475 μs). The top to bottom interferograms correspond to the lowest to highest frequency lines in the spectra of Figure 2.

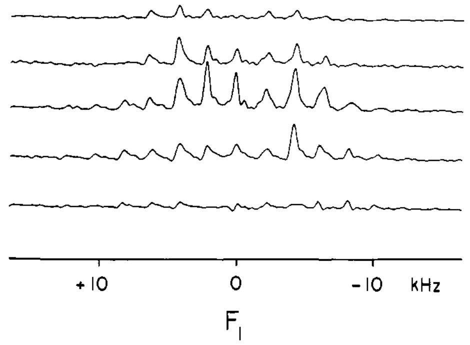

Figure 4. Cross sections through the two-dimensional chemical shift-dipolar spectrum corresponding to the centerband and sidebands of the chemical shift dimension. These phase-sensitive traces are obtained by Fourier transformation of the interferograms in Figure 3.

Figure 2 shows preliminary spectra obtained using the pulse sequence in Figure 1a from a sample of $Ca(CHO_2)_2$ as a function of t_1. These spectra exhibit a modulation due to the CH dipolar interactions discussed above. The amplitudes of the peaks of the

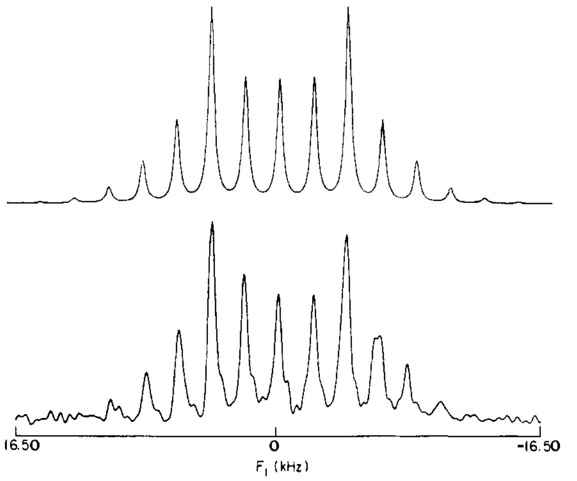

Figure 5. CH dipolar spectra under conditions of magic angle sample rotation. Top: calculated spectrum resulting from a scaled dipolar coupling of 23 kHz and a rotation frequency of 2.15 kHz. Bottom: experimental dipolar projection obtained by summing up all cross-sections in the F_1 domain.

centerband and sidebands in Figure 2 are plotted as a function of t_1 in Figure 3 where it is apparent that a train of rotational echoes occurs in the dipolar t_1 dimension. The echoes reflect the fact that the destructive interference due to the time-dependent dipolar splitting is removed when all crystallites have undergone an integral number of sample revolutions. Since rotational echoes now occur in both the chemical shift and dipolar dimensions, we refer to this type of experiment as "two-dimensional rotational spin–echo NMR".

A second Fourier transformation with respect to t_1 yields a two-dimensional spectrum correlating the chemical shift anisotropy with the heteronuclear dipolar splittings. Cross sections corresponding to the sidebands in the chemical shift dimension are shown in Figure 4, and we now see that sidebands occur in both dimensions as a result of rotational echoes. Note that the cross sections shown in Figure 4, which corresponds to an intermediate spinning regime, show features discussed above for the limits of fast and slow rotation. For example, the F_1 slice due to the centerband in the chemical shift dimension is beginning to assume the shape of a Pake doublet. At the same time, the sidebands in the shift dimension reveal dipolar spectra resulting from a weighted average which favors selected sets of crystallites.

Projection of the sidebands onto the F_2 shift axis results in the normal shift anisotropy spinning pattern. This is easily understood in terms of the theorem of Fourier analysis which equates the integrated area of a frequency spectrum with the magnitude of the first point in the time domain. On the other hand, the dipolar projection onto the F_1 axis shown at the bottom of Figure 5 is symmetric and represents a *Pake pattern free of shift anisotropy effects.* This is invariably the result even though intensity

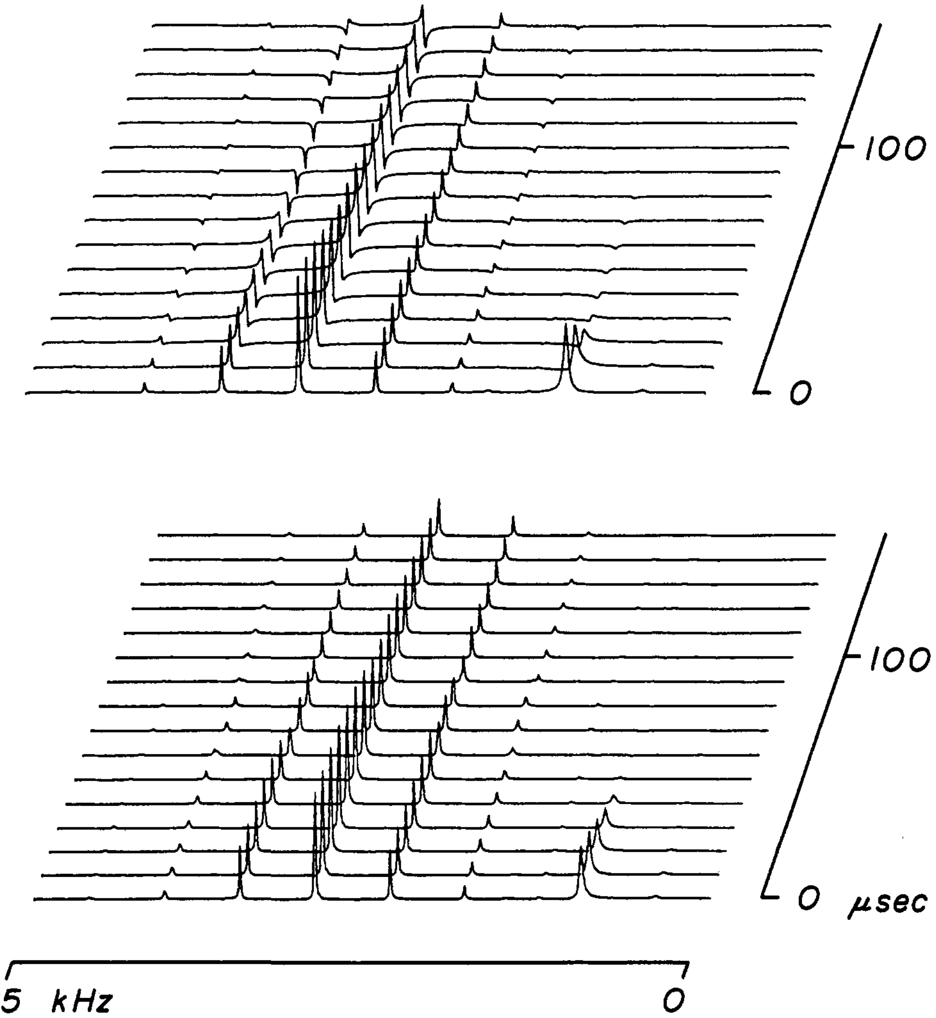

Figure 6. ^{13}C MASS spectra of glycine, $NH_3^+CH_2CO_2^-$, illustrating the suppression of protonated ^{13}C resonances. Top: Spectra obtained by simply inserting a delay between cross-polarization and the simultaneous initiation of sampling and application of ^1H decoupling. Note the frequency-dependent phase shifts in the sideband manifold of the $-CH_2-$ resonance and between the $-CO_2^-$ and $-CH_2-$ centerbands. Bottom: spectra obtained with the pulse sequence of Figure 1c. These spectra are free of linear phase distortions since both isotropic and anisotropic shifts are refocused by this pulse sequence. The $-CH_2-$ line on the right disappears after about 50 μs. The ratio of the integrated intensities of the lines in the $t_1 = 0$ spectrum is not 1:1 because the sample contained unequal amounts of carboxyl- and methylene-enriched glycine.

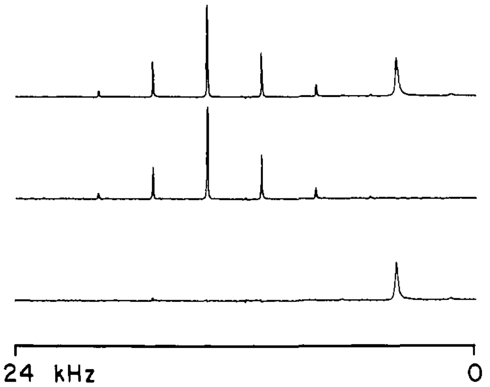

Figure 7. Glycine spectra from Figure 6 for $t_1 = 0$ (top) and $t_1 = 100$ μs (middle) and their weighted difference (bottom). The centerband and sidebands on the left are due to the $-CO_2-$ while those on the right arise from the $-CH_2-$. Note the clean separation of the resonances due to protonated and nonprotonated ^{13}C's.

asymmetries are observed for certain shift-dipolar sidebands as a result of the averaging process in a rotating sample. Shown in the top half of Figure 5 is a calculated dipolar spectrum which was obtained by assuming an effective CH coupling of 23.0 kHz and a rotation rate of 2.15 kHz. Additional simulations indicate that variations in bond distances of 0.01 Å should be detectable, particularly if least-squares methods are used to fit the relative intensities of the sidebands.[24] The present result, however, is uncertain by 3% and yields an internuclear separation of 1.15 Å if the WAHUHA scaling factor is taken to be $1/\sqrt{3}$.[25] The apparently long bond length is consistent with the results of Stoll et al.[11] who concluded that molecular motion at room temperature narrows the dipolar spectrum of β-calcium formate. Equivalent dipolar information would be difficult to extract using one-dimensional NMR techniques since it is not possible to remove the chemical shift anisotropy while retaining the dipolar coupling. The technique described here is applicable to systems with an arbitrary number of inequivalent ^{13}C sites, provided the isotropic shifts do not overlap.

IV. Selection of Protonated and Nonprotonated Resonances

An interesting special case of this experiment occurs when protonated and nonprotonated carbons are present simultaneously in the sample. In this situation the dipolar coupling causes a rapid decay of the protonated ^{13}C magnetization for increasing t_1, whereas for nonprotonated species this process is much slower. This is apparent in the rotational echo trains shown in Figure 3 where for $50 \leq t_1 \leq 500$ μs the dipolar modulation has severely attenuated the signal. Fourier transformation of the decay of a properly selected t_1 value will yield the spectrum of the nonprotonated ^{13}C's in a manner similar to the one recently demonstrated by Opella and Frey.[26] This is illustrated in Figure 6 with spectra of glycine ($NH_3^+-CH_2-CO_2^-$) obtained as a function of t_1 using differing methods which emphasize the benefits of refocusing pulses. In particular, the spectra in the top half of this figure were recorded with sequence 1a without rotational synchronization of data acquisition and without homonuclear decoupling. While this experiment does indeed suppress the protonated ^{13}C line, it also induces large linear phase distortions in the CO_2^- sideband manifold and between the $-CO_2^-$ and $-CH_2-$ centerbands as well. Incorporation of the refocusing features discussed above eliminates the phase shifts, as is shown in the bottom half of Figure 6. These spectra were taken with sequence 1c, again without application of a multiple-pulse sequence to the protons in order to hasten the decay of the magnetization arising from protonated carbon atoms. Here the spectra show proper absorption-mode phases for all centerbands and sidebands since both isotropic and anisotropic shifts are refocused with this sequence. Consequently, it is easy to obtain difference spectra which retain only the protonated resonances. An example is shown in Figure 7 where the $t = 0$ spectrum (top) shows the centerbands and sidebands from both ^{13}C resonance; the $t = 100$ μs spectrum (middle) shows only the $-CO_2^-$ resonance. Thus, in situations where rotational sidebands are present and the sampling rate is comparable to or greater than the t_1 period in the experiment, the pulse sequence of Figure 1c would appear to be the preferred approach to differentiating between resonances of protonated and nonprotonated S spins.

V. Summary

The experiments outlined here provide a means to obtain high-resolution dipolar spectra from powder samples in the absence of chemical shift anisotropy. In principle, these spectra permit a determination of the relative orientations of the chemical shift and dipolar interactions as well as the principal values of these two tensors. The dipolar tensor yields information on I–S distances and consequently it would appear that this technique provides a general method for determining these structural parameters in powders. A simple application of the experiment allows the differentiation of protonated and nonprotonated carbon resonances. Finally, although we have demonstrated the technique for $^{13}C-^1H$ spin pairs, it should be applicable to a variety of other cases so long as the Hamiltonians of the nuclear species involved are inhomogeneous.

VI. Experimental Section

The experiments were performed on a home-built pulse spectrometer operating at 294 MHz for ^1H and 74 MHz for ^{13}C. The spinning probe employed Kel-F Andrew-Beam-type rotors with spinning rates in the neighborhood of 2–3 kHz.[27] Proton and carbon rotating rf fields were approximately 10 and 40 G, respectively. $Ca(CHO_2)_2$ samples were enriched to 30% and light doping with Mn^{2+} was used to shorten the proton T_1. The preparation involved evaporation of an aqueous solution at elevated temperatures, a condition which favors the formation of the β phase of this compound.[28] Glycine spectra were obtained from a mixture of 1 and 2 position labeled species enriched to approximately 30%.

Acknowledgment. This research was supported by the National Institutes of Health through Grants GM-23403, GM-23289, GM-26272, and RR-00995 and by the National Science Foundation through Contract C-670 to the Francis Bitter National Magnet Laboratory. We are grateful to C. M. Dobson and W. P. Aue for helpful comments.

---

(23) The complex magnetization arising from a given orientation is proportional to $\cos \theta_{DIP}(t_1)\, e^{i\theta_{CS}(t_2)}$, where $\theta_{DIP}(t_1)$ and $\theta_{CS}(t_2)$ refer to the accumulated phase angles due to the dipolar and shift interactions, respectively. These phase angles are simply time integrals of the appropriate Hamiltonian expressed in units of angular frequency. The necessary expressions are tabulated in the paper by Maricq and Waugh.[17]

(24) J. Herzfeld and A. E. Berger, *J. Chem. Phys.*, **73**, 6021 (1980).

(25) The scaling factor in multiple-pulse experiments is strongly dependent on rf pulse width and phase and on rf homogeneity. Since none of these parameters were optimized, this instrumental constant presents the largest single contribution to the uncertainty of the reported result.

(26) S. J. Opella and M. H. Frey, *J. Am. Chem. Soc.*, **101**, 5854 (1979). The pulse sequence described in this paper was evidently first used by Alla and Lippmaa to measure T_2 for individual ^{13}C's in a static sample: M. Alla and E. Lippmaa, *Chem. Phys. Lett.*, **37**, 260 (1976).

(27) E. R. Andrew, *Prog. NMR Spectrosc.*, **8**, 1 (1971).

(28) M. Matsui, T. Watanabe, N. Kamijo, R. L. Lapp, and R. A. Jacobson, *Acta Crystallogr., Sect. B*, **36**, 1081–1086 (1980).